Transmitochondrial mito-mice Δ and mtDNA mutator mice, but not aged mice, share the same spectrum of musculoskeletal disorders

著者別名	石川 香, 中田 和人, 林 純一
journal or publication title	Biochemical and biophysical research communications
volume	456
number	4
page range	933-937
year	2015-01
権利	(C) 2014 Elsevier Inc. NOTICE: this is the author's version of a work that was accepted for publication in Biochemical and biophysical research communications. Changes resulting from the publishing process, such as peer review, editing, corrections, structural formatting, and other quality control mechanisms may not be reflected in this document. Changes may have been made to this work since it was submitted for publication. A definitive version was subsequently published in Biochemical and biophysical research communications, 456,4,2015. doi:10.1016/j.bbrc.2014.12.009
URL	http://hdl.handle.net/2241/00123580

doi: 10.1016/j.bbrc.2014.12.009

Transmitochondrial mito-miceΔ and mtDNA mutator mice, but not aged mice, share the same spectrum of musculoskeletal disorders

Takayuki Mito[a], Hikari Ishizaki[a], Michiko Suzuki[a], Hitomi Morishima[a], Azusa Ota[a], Kaori Ishikawa[a], Kazuto Nakada[a, b], Akiteru Maeno[c], Toshihiko Shiroishi[c], and Jun-Ichi Hayashi [a, b, d]

[a] Faculty of Life and Environmental Sciences, University of Tsukuba, Tsukuba, Ibaraki, Japan.

[b] International Institute for Integrative Sleep Medicine (WPI-IIIS), University of Tsukuba, Tsukuba, Ibaraki, Japan.

[c] Mammalian Genetics Laboratory, National Institute of Genetics, Mishima, Shizuoka, Japan

[d] TARA Center, University of Tsukuba, Tsukuba, Ibaraki 305-8572, Japan.

[1]To whom correspondence should be addressed:
Tel. +81-298-53-6650;
Fax. +81-298-53-6614;
e-mail: jih45@biol.tsukuba.ac.jp

Key words: mtDNA mutator mice, mito-miceΔ, mitochondrial diseases, aging, osteoporosis, sarcopenia

ABSTRACT

The spectra of phenotypes associated with aging and mitochondrial diseases sometimes appear to overlap with each other. We used aged mice and a mouse model of mitochondrial diseases (transmitochondrial mito-miceΔ with deleted mtDNA) to study whether premature aging phenotypes observed in mtDNA mutator mice are associated with aging or mitochondrial diseases. Here, we provide convincing evidence that all the mice examined had musculoskeletal disorders of osteoporosis and muscle atrophy, which correspond to phenotypes prevalently observed in the elderly. However, precise investigation of musculoskeletal disorders revealed that the spectra of osteoporosis and muscle atrophy phenotypes in mtDNA mutator mice were very close to those in mito-miceΔ, but different from those of aged mice. Therefore, mtDNA mutator mice and mito-miceΔ, but not aged mice, share the spectra of musculoskeletal disorders.

1. Introduction

Human mtDNA with pathogenic mutations that induce mitochondrial respiration defects has been proposed to cause mitochondrial diseases, and could also be involved in aging

[1-5]. This concept (mitochondria theory of aging) is supported by studies in mtDNA mutator mice [6, 7]. In these mice, proofreading-defective mtDNA polymerase enhances accumulation of somatic mtDNA mutations and leads to age-associated respiration defects and various premature aging phenotypes.

In contrast, our previous studies revealed that age-associated respiration defects found in human fibroblasts are caused not by mtDNA mutations [8, 9] but by nuclear-recessive mutations [9]. Moreover, transmitochondrial mito-mice carrying mtDNA with a large-scale deletion (mito-miceΔ) showed age-associated accumulation of the mutated mtDNA and the resultant expression of phenotypes of mitochondrial diseases, but had no premature aging phenotypes [10, 11]. Therefore, it appeared to be controversial that mtDNA mutator mice, but not mito-miceΔ, express premature aging phenotypes, even though both mice express age-associated respiration defects due to age-associated accumulation of mtDNA with mutations.

Our subsequent study [12] revealed that the apparent discrepancy was partly due to the differences in the nuclear genetic backgrounds of mtDNA mutator mice and mito-

miceΔ: by generating mtDNA mutator mice that share the same C57BL/6J (B6J) nuclear genetic background as that of mito-miceΔ, we showed that both mouse models commonly exhibit premature aging phenotypes of kyphosis and a short lifespan, but do not express premature aging phenotypes of graying and alopecia [12]. Thus, the spectra of abnormalities in the mtDNA mutator mice with a B6J nuclear background are very similar to those of mito-miceΔ that express phenotypes of mitochondrial diseases [10, 11].

The question that then arises is whether mtDNA mutator mice correspond to a model of aging or mitochondrial diseases. Here we addressed this issue by using aged mice and mito-miceΔ as positive controls for aging and mitochondrial diseases, respectively, and investigated precisely musculoskeletal disorders, including osteoporosis and muscle atrophy, which have been reported in elderly human subjects [13] and mtDNA mutator mice [6, 7].

2. Materials and methods

*2.*1. Mice

Inbred B6J mice generated by sibling mating more than 40 times were obtained from CLEA Japan. Mito-miceΔ and mtDNA mutator mice were generated in our previous studies [10, 12]. Animal experiments were performed in accordance with protocols approved by the Experimental Animal Committee of the University of Tsukuba, Japan.

2.2. Micro-computed tomography analysis

The μ-CT (Scan X mate E090S scanner, Comscantechno, Kanagawa, Japan) was used to take tomography images at three parts in mouse tibia bones. The μ-CT was operated at a tube voltage peak of 90 kV and a tube current of 90 mA. Samples were rotated 360° in steps of 0.6°, generating 600 projection images of 992 × 992 pixels. The μ-CT data were reconstructed at an isotropic resolution of 22.4×22.4×22.4 mm^3 (the wide part of tibia) and 7×7×7 mm^3 (the proximal metaphysis and the mid-diaphysis). 0.1mm brass filter was used for the scanning of the wide part of tibia and the mid-diaphysis. For each analysis, the region of interest (ROI) was defined on the basis of an anatomical feature (Fig. S1). Morphometric indices were calculated using TRI/3D-BON (RATOC System

Engineering, Tokyo, Japan) software. Bone mineral density of tibia bones were measured using TRI/3D-BON-BMD (RATOC Systems) software.

2.3. Quantitative RT-PCR

Total RNA was extracted from mouse quadriceps muscles by using the RNeasy fibrous mini kit (Qiagen, Hilden, Germany). RNA samples were reverse transcribed by using QuantiTect Reverse Transcription Kit (Qiagen). Real-time monitoring PCR was performed with QuantiTect SYBR Green PCR Kit (Qiagen), an ABI PRISM 7900HT sequence detection system (Applied Biosystems, CA, USA), and primers for atrogin-1 (forward, ctctgtaccatgccgttcct; reverse, ggctgctgaacagattctcc) and TATA-box binding protein (forward, ggcggtttggctaggttt; reverse: gggttatcttcacacaccatga). The relative expression level of *atrogin-1* mRNA was calculated by using ΔΔCt method. The gene encoding TATA-box binding protein was used as an internal control. The proportion of wild type mtDNA and ΔmtDNA was determined by real-time PCR analysis, as described previously [12].

2.4. Ex vivo differentiation of osteoclasts and osteoblasts

Bone marrow macrophages were induced by incubating bone marrow flushed from mouse femurs and tibiae with macrophage inducing medium: MEMα Glutamax (Gibco, CA, USA) containing 10% fetal bovine serum (FBS) and 10 ng/mL recombinant macrophage colony stimulating factor 1 (M-CSF) (Wako, Osaka, Japan), and purified by Ficoll-Hypaque (GE Healthcare, Buckinghamshire, UK) gradient centrifugation. Osteoclasts were induced by incubating bone marrow macrophages in MEMα Glutamax containing 10% FBS, 50 ng/mL recombinant M-CSF, and 100ng/mL recombinant receptor activator of nuclear factor kappa-B ligand (RANKL) (Wako) for 5 days. Pre-osteoblasts were selected from bone marrow by incubating whole bone marrow cells in RPMI1640 (Nissui, Tokyo, Japan) containing 10% FBS for 7 days. Osteoblasts were induced by incubating pre-osteoblasts in RPMI1640 containing Osteoblast-Inducer Reagent (TaKaRa, Shiga, Japan) for 14 days. Cytochemical analysis of cytochrome *c* oxidase (COX) activity of osteoclasts and osteoblasts was performed as described previously [12].

2.5. Histological Analyses

Frozen sections (10-µm) of quadriceps muscles were used for COX and H&E staining, as described previously [12]. Cross sectional area (CSA) of skeletal muscle fibers was calculated from H&E stained section by using ImageJ (Rasband, WS., Image J, U.S. National Institutes of Health, Bethesda, Maryland, USA, http://imagej.nih.gov/ij/, 1997-2014) software.

2.6. Statistical Analysis

Data were analyzed by two-sided Student's *t*-test. *P* values of less than 0.05 were considered significant.

3. Results

First we compared bone mineral density (BMD) in aged mice, mtDNA mutator mice, and mito-miceΔ, because decreased BMD is an osteoporosis phenotype prevalent in elderly human subjects and a phenotype observed in mtDNA mutator mice. We carried out quantitative estimation of BMD in tibia bones (Fig. S1A), and showed that its expression was significantly decreased in aged mice, mtDNA mutator mice, and mito-miceΔ compared with young mice (Fig. 1A).

For further investigation of the structural abnormalities associated with the decreased BMD (Fig. 1B), we performed X-ray micro-computed tomography (μ-CT) analysis of trabecular and cortical bones (Fig. S1B and C). Quantitative estimation of trabecular bone volume (Fig. 1C) and cortical bone thickness (Fig. 1D) showed that cortical bone thickness, but not trabecular bone volume, decreased in both mtDNA mutator mice and mito-miceΔ; in contrast, aged mice did not show a significant decrease in either trabecular bone volume or cortical bone thickness. Together with the finding that elderly human subjects exhibit a decrease in trabecular bone volume but not cortical bone thickness [14], our result suggests that decreased cortical bone thickness exclusively found in mtDNA mutator mice and mito-miceΔ is not associated with either mouse or human aging.

We then compared respiratory function by using osteoclasts and osteoblasts, which play an important role in bone metabolism. Cytochemical analysis of mitochondrial cytochrome *c* oxidase (COX) activity showed reduced activity in the cells of mtDNA mutator mice and mito-miceΔ, but not in the cells of aged mice, when compared with young mice (Fig. 1E). These results indicate that the decreased BMD (Fig. 1A) and

cortical bone thickness (Fig. 1D) observed in mtDNA mutator mice and mito-miceΔ are likely due to respiration defects, whereas the decreased BMD observed in aged mice (Fig. 1A) occurred in the absence of the respiration defects (Fig. 1E).

Next, we investigated muscle atrophy, another typical aging phenotype of musculoskeletal disorders, which is observed not only in elderly human subjects [13] and mtDNA mutator mice [6, 7], but also in patients with mitochondrial diseases [15], cachexia, or sepsis [16]. By isolating and measuring the weight of quadriceps muscles (Fig. 2A and B), we observed muscle atrophy in aged mice, mtDNA mutator mice, and mito-miceΔ compared with young mice. Furthermore, histochemical analysis also showed atrophy of each muscle fiber (Fig. 2C and D), which confirmed the presence of muscle atrophy in the quadriceps of all three mouse models.

Comparison of the mitochondrial respiratory function of quadriceps was performed by histochemical analysis of COX activity. Decreased COX activity relative to that in young mice was observed in muscle fibers of mtDNA mutator mice and mito-miceΔ, but not in aged mice (Fig. 2E). Therefore, mitochondrial respiration defects could be

responsible for the muscle atrophy expressed in mtDNA mutator mice and mito-miceΔ, whereas aged mice had muscle atrophy in the absence of the respiration defects. Decreased COX activity in muscle fibers corresponds to mitochondrial myopathy, which is one of the typical abnormalities frequently observed in patients with mitochondrial diseases [1, 4]. Therefore, mtDNA mutator mice and mito-miceΔ also share a phenotype associated with mitochondrial diseases.

For further investigation of muscle atrophy, we examined *atrogin*-1 mRNA levels, because overexpression of the *atrogin*-1 gene, which encodes an E3 ubiquitin ligase involved in proteolysis, is observed in human muscle atrophy caused by cachexia, sepsis, or immobilization [16], but not in age-associated muscle atrophy (sarcopenia) developed in the elderly [17]. Here we observed that *atrogin*-1 mRNA was overexpressed in quadriceps of both mtDNA mutator mice and mito-miceΔ, but not in aged mice, relative to the levels in young mice (Fig. 2F). These observations suggest that the mechanisms behind muscle atrophy in mtDNA mutator mice are similar to those in mito-miceΔ, but differ from those in aged mice and elderly human subjects, that develop muscle atrophy in the absence of *atrogin*-1 overexpression.

4. Discussion

The mitochondrial theory of aging [1-5] proposes a vicious cycle of age-associated accumulation of somatic mutations in mtDNA and the resultant respiration defects and overproduction of reactive oxygen species (ROS). This concept was partly supported by studies in mtDNA mutator mice, which had premature aging phenotypes along with the accumulation of somatic mutations in mtDNA, although they did not display ROS overproduction [7, 18]. However, mito-miceΔ showing age-associated accumulation of the mutated mtDNA and the resultant respiration defects had no premature aging phenotypes [10, 11]. We addressed to the controversial issue that mtDNA mutator mice, but not mito-miceΔ, express premature aging phenotypes, and revealed that decreased cortical bone thickness (Fig. 1D) and overexpression of *atrogin*-1 in muscle atrophy (Fig. 2F) were exclusively observed in mtDNA mutator mice and mito-miceΔ, but not in aged mice.

Therefore, the spectra of musculoskeletal disorders in mtDNA mutator mice and mito-miceΔ are similar to each other, but different from those in aged mice. Considering that

the spectra of musculoskeletal disorders in mtDNA mutator mice and mito-miceΔ are also different from those in elderly human subjects [14, 17], they would not be associated with either mouse or human aging. Then, a question that arises is whether decreased cortical bone thickness and increased *atrogin*-1 mRNA expression in muscle fibers are associated with mitochondrial diseases. To answer this question, further works are required to investigate whether the patients with mitochondrial diseases express these abnormalities.

Conflict of interest

The authors have no conflict of interest.

Acknowledgments

This work was supported by Grants-in-Aid for Scientific Research (A) (No. 23240058 and No. 25250011) from the Ministry of Education, Culture, Sports, Science and Technology of Japan (MEXT) to KN and JIH, respectively. This work was also supported by a Grant-in-Aid for Japan Society for the Promotion of Science (JSPS) Fellows (No. 26-467) to TM.

References

[1] Wallace DC (1999) Mitochondrial diseases in man and mouse. Science 283, 1482–1488.

[2] Jacobs HT (2003) The mitochondrial theory of aging: dead or alive? Aging Cell 2, 11–17.

[3] Loeb LA, Wallace DC, Martin GM (2005) The mitochondrial theory of aging and its relationship to reactive oxygen species damage and somatic mtDNA mutations. Proc Natl Acad Sci U S A 102, 18769–18770.

[4] Taylor RW, Turnbull DM (2005) Mitochondrial DNA mutations in human disease. Nat Rev Genet 6, 389–402.

[5] Khrapko K, Vija J (2009) Mitochondrial DNA mutations and aging: devils in the details? Trends Genet 25, 91–98.

[6] Trifunovic A, Wredenberg A, Falkenberg M, Spelbrink JN, Rovio AT, Bruder CE, Bohlooly YM, Gidlof S, Oldfors A, Wibom R, Tornell J, Jacobs HT, Larsson NG (2004) Premature ageing in mice expressing defective mitochondrial DNA polymerase. Nature 429, 417–423.

[7] Kujoth GC, Hiona A, Pugh TD, Someya S, Panzer K, Wohlgemuth SE, Hofer T, Seo AY, Sullivan R, Jobling WA, Morrow JD, Van Remmen H, Sedivy JM, Yamasoba T, Tanokura M, Weindruch R, Leeuwenburgh C, Prolla TA (2005) Mitochondrial DNA mutations, oxidative stress, and apoptosis in mammalian aging. Science 309, 481–484.

[8] Hayashi J, Ohta S, Kagawa Y, Kondo H, Kaneda H, Yonekawa H, Takai D, Miyabayashi S (1994) Nuclear but not mitochondrial genome involvement in human age-related mitochondrial dysfunction. J Biol Chem 269, 6878.

[9] Isobe K, Ito S, Hosaka H, Iwamura Y, Kondo H, Kagawa Y, Hayashi J-I (1998) Nuclear-recessive mutations of factors involved in mitochondrial translation are responsible for age-related respiration deficiency of human skin fibroblasts. J Biol Chem 273, 4601.

[10] Inoue K, Nakada K, Ogura A, Isobe K, Goto Y-I, Nonaka I, Hayashi J-I. (2000) Generation of mice with mitochondrial dysfunction by introducing mouse mtDNA carrying a deletion into zygotes. Nat Genet 26, 176–181.

[11] Nakada K, Inoue K, Ono T, Isobe K, Ogura A, Goto Y-I, Nonaka I, Hayashi J-I (2001) Inter-mitochondrial complementation: Mitochondria-specific system preventing mice from expression of disease phenotypes by mutant mtDNA. Nat Med 7, 934-940.

[12] Mito T, Kikkawa Y, Shimizu A, Hashizume O, Katada S, Imanishi H, Ota A, Kato Y, Nakada K, Hayashi J-I (2013) Mitochondrial DNA mutations in mutator mice confer respiration defects and B-cell lymphoma development. PLoS ONE 8. e55789.

[13] Nedergaard A, Henriksen K, Karsdal MA, Christiansen C (2013) Musculoskeletal ageing and primary prevention. Best Pract Res Clin Obstet Gynaecol 27, 678-688

[14] Rosenberg AE (1991) The pathology of metabolic bone disease. Radiol Clin North Am 29, 19-36

[15] Cohen BH (2013) Neuromuscular and systemic presentations in adults: diagnoses beyond MERRF and MELAS. Neurotherapeutics 10, 227-242

[16] Foletta VC, White LJ, Larsen AE, Leger B, Russell AP (2011) The role and regulation of MAFbx/atrogin-1 and MuRF1 in skeletal muscle atrophy. Pflugers Arch 461, 325-335

[17] Sakuma K, Aoi W, Yamaguchi A. (2014) The intriguing regulator of muscle mass in sarcopenia and muscular dystrophy. Front Aging Neurosci 6, 230

[18] Trifunovic A, Hansson A, Wredenberg A, Rovio AT, Dufour E, Khvorostov I, Spelbrink JN, Wibom R, Jacobs HT, Larsson NG (2005) Somatic mtDNA mutations cause aging phenotypes without affecting reactive oxygen species production. Proc Natl Acad Sci U S A 102, 17993–17998.

Figure legends

Fig. 1. Characterization of phenotypes of osteoporosis displayed in tibia bones of mtDNA mutator mice. Aged mice and mito-miceΔ were used as controls expressing phenotypes associated with aging and mitochondrial diseases, respectively. All mice were males sharing the B6J nuclear genetic background. Young, 10-month-old mice; Aged, 27-month-old mice; Mutator, 10-month-old mtDNA mutator mice; Delta, 10-month-old mito-mice Δ. The proportions of ΔmtDNA in the tail from mito-miceΔ were 57.5 ± 2.5 % at 4 weeks after birth and 81.2 ± 1.3 % at 10 months old. (A) Quantitative estimation of BMD. Data are means ± SD. *, $P < 0.05$ ($n = 3$). (B) µ-CT analysis of trabecular and cortical bones. Upper panel, red-colored areas correspond to trabecular bones; lower panel, bone areas exclusively consisting of cortical bones (gray-colored

areas). Scale bar, 500 μm. (C) Quantitative estimation of the ratio of trabecular bone volume/ tissue volume (BV/TV). Data are means ± SD. *, $P < 0.05$ ($n = 3$). (D) Quantitative estimation of cortical bone thickness (Ct). Data are means ± SD. *, $P < 0.05$ ($n = 3$). (E) Cytochemical analysis of COX activity. OCs, osteoclasts; OBs, osteoblasts. Cells that had lost their COX activity were detected as a blue color. The proportions of ΔmtDNA in the bone marrow cells, osteoclasts, and osteoblasts were 65.1 %, 61.5 %, and 57.7 %, respectively. Scale bars, 50 μm.

Fig. 2. Characterization of phenotypes of muscle atrophy displayed in quadriceps of mtDNA mutator mice. Aged mice and mito-miceΔ were used as controls of phenotypes associated with aging and mitochondrial disease, respectively. All mice were males sharing the B6J nuclear genetic background. Young, 10-month-old mice; Aged, 27-month-old mice; Mutator, 10-month-old mtDNA mutator mice; Delta, 10-month-old mito-mice Δ. (A) Images of whole quadriceps. The proportions of ΔmtDNA in the quadriceps from mito-miceΔ were 82.6 %. Scale bar, 5 mm. (B) Tissue weights of quadriceps. The proportions of ΔmtDNA in the quadriceps muscles from mito-miceΔ were 83.1 ± 2.2 %. Data are means ± SD. *, $P < 0.05$ ($n = 3$). (C) Hematoxylin and eosin (H&E) staining of muscle fibers in quadriceps. The proportions of ΔmtDNA in the quadriceps from mito-miceΔ were 83.2 %. Scale bar, 50 μm. (D) Quantitative estimation of cross-sectional areas (CSA) of each muscle fiber. The proportions of ΔmtDNA in the quadriceps muscles from mito-miceΔ were 82.9 ± 2.1 %. Data are means ± SD. *, $P < 0.05$. (E) Histochemical analysis of COX activity in quadriceps.

The intensity of brown-staining represents the level of COX activity. The proportions of ΔmtDNA in the quadriceps from mito-miceΔ were 82.7 %. Scale bar, 50 μm. (F) Estimation of the mRNA levels of *atrogin*-1 in quadriceps by using quantitative real-time PCR. The proportions of ΔmtDNA in the quadriceps muscles from mito-miceΔ were 83.0 ± 1.8 %. Data are means ± SD. *, $P < 0.05$ ($n = 4$).

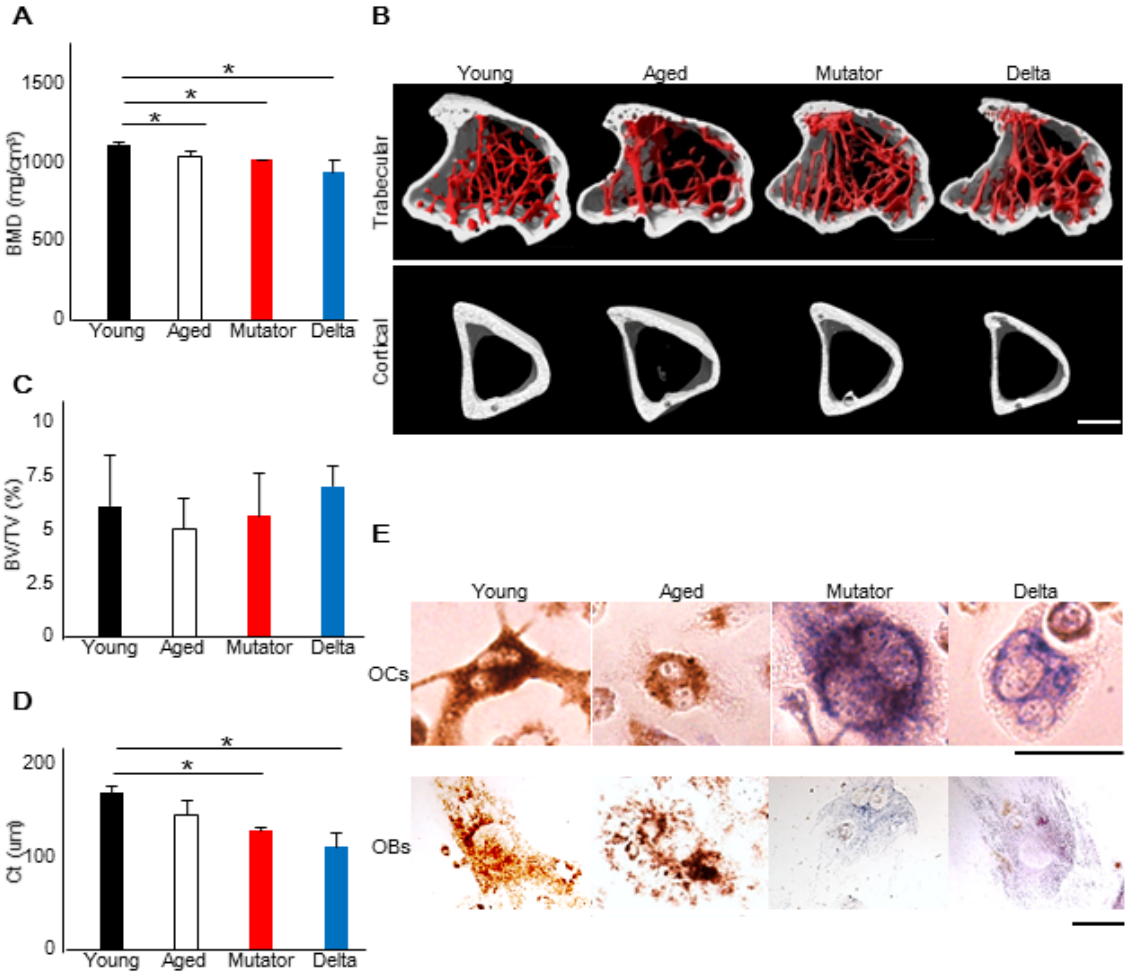

Mito et al, Fig. 1

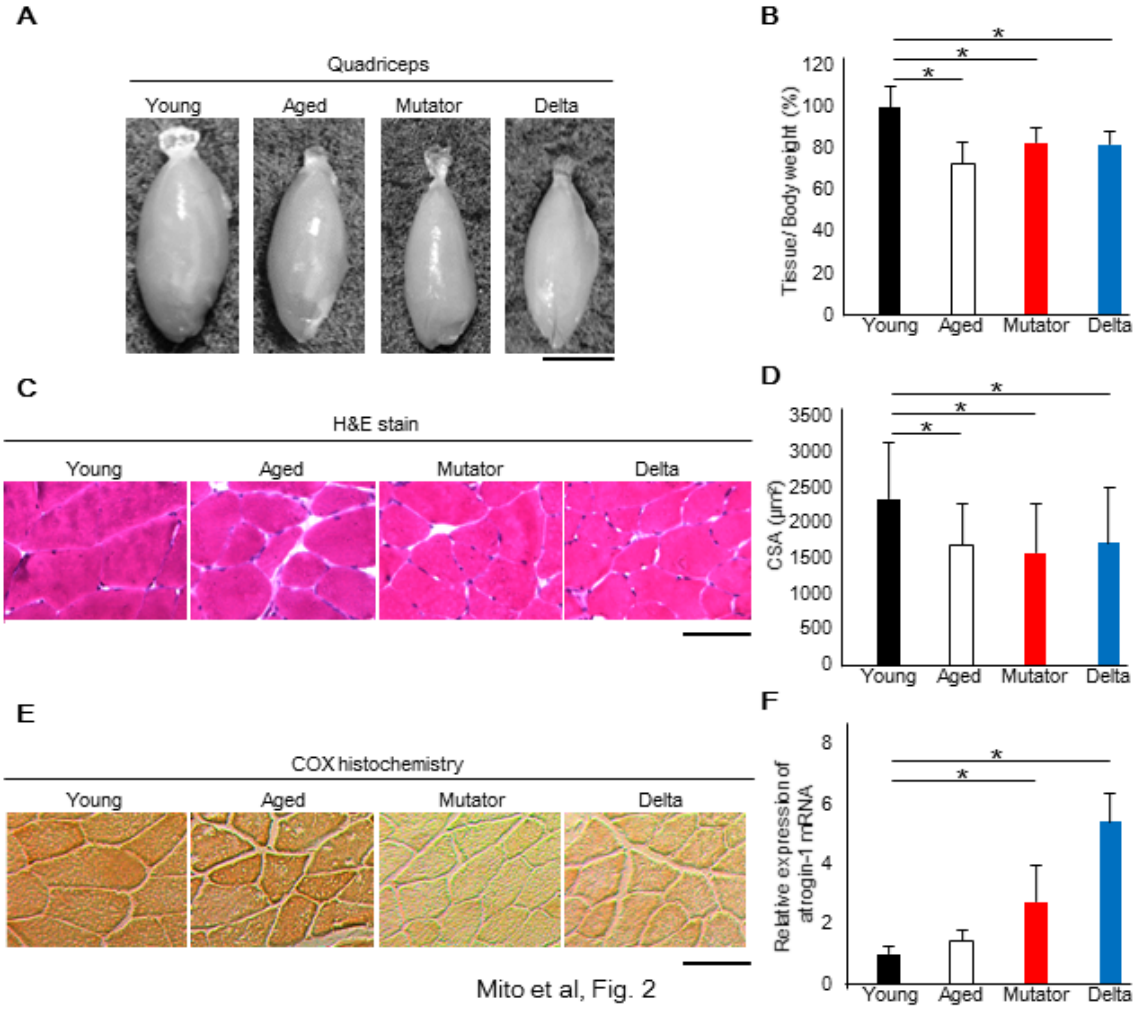

Mito et al, Fig. 2

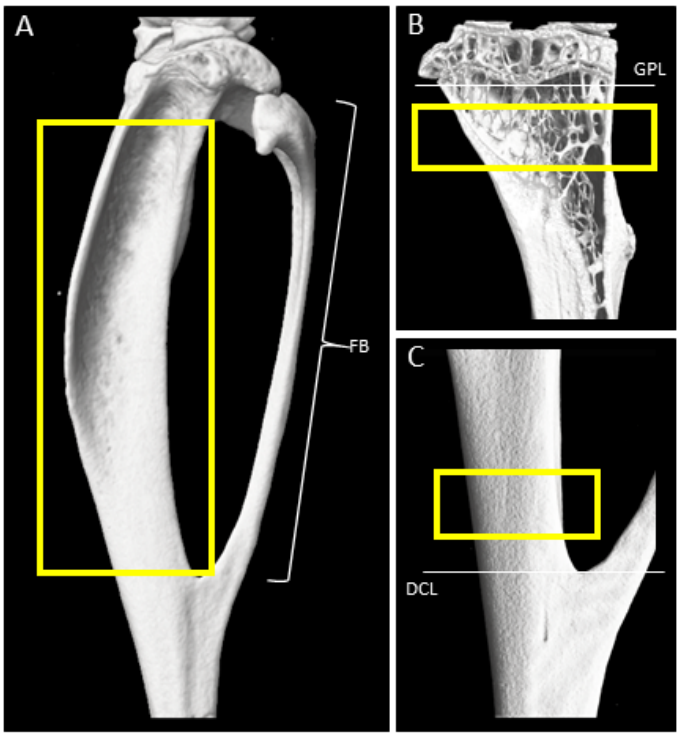

Figure S1. Three-dimensional images showing the ROI for each analysis. A, Wide part of tibia. Yellow-square region (between two connection points to fibula bone; FB) was defined as the ROI for BMD analysis. **B**, Proximal metaphysis of tibia. Yellow-square region (1mm in length from 0.4 mm below the line of proximal growth plate; GPL) was defined as the ROI for trabecular bone analysis. **C**, Mid-diaphysis of tibia. Yellow-square region (2mm in length from 1mm above the line of the distal connection point to fibula; DCL) was defined as the ROI for cortical bone analysis.